RSC Advances

PAPER

View Article Online
View Journal | View Issue

Cite this: *RSC Adv.*, 2025, **15**, 50784

Effects of different carbon-to-nitrogen (C/N) ratios and dissolved oxygen (DO) concentrations on denitrification performance and structure of microbial community in a moving bed biofilm reactor (MBBR)

Jing-Rui Yang, *[a] Shan-Shan Duan[b] and Chun-Fang Wu[a]

This study elucidated the synergistic regulatory mechanism of carbon-to-nitrogen ratio (C/N) and dissolved oxygen (DO) concentration on the nitrogen removal performance in a moving bed biofilm reactor (MBBR). It was innovatively discovered that the matching relationship between C/N and DO is a key factor determining system performance: when a low C/N (=5) was matched with low DO (0.6 mg L^{-1}), or a high C/N (=12) was matched with high DO (3 mg L^{-1}), excellent nitrogen removal was achieved, with COD and nitrate removal efficiencies as high as 97.1%/99.0% and 96.3%/100%, respectively. The nitrogen balance and enzyme activity experiments demonstrated that the removal of nitrate partially relies on the assimilation of microorganisms, converting it into biomass nitrogen required for microbial growth, while the other part is converted into N_2 through denitrification. The study confirmed the recognition that the microbial community's demand for C/N is positively correlated with DO concentration. High-throughput sequencing revealed that when the C/N–DO matching was imbalanced (*e.g.*, C/N = 5, DO = 3 mg L^{-1}), significant shifts in the dominant phyla occurred: the relative abundance of *Proteobacteria* dropped sharply from over 72% to 47.35%, while that of *Bacteroidetes* increased to 50.95%, directly leading to a decrease in nitrate removal efficiency to 68.6%. This study confirms that precise regulation of C/N–DO combinations can directionally shape the microbial community structure, providing an innovative theoretical basis for achieving precise regulation of MBBR process.

Received 27th March 2025
Accepted 12th December 2025

DOI: 10.1039/d5ra02142a

rsc.li/rsc-advances

1 Introduction

Nitrate nitrogen pollution, primarily from excessive fertilizer use, untreated industrial/domestic wastewater, and atmospheric deposition, poses significant threats to ecosystems and human health.[1] It acts as a key contributor to eutrophication, triggering algal blooms that deplete oxygen and create "dead zones" in aquatic environments. For humans, nitrate in drinking water is converted to nitrite, which can cause methemoglobinemia ("blue baby syndrome") in infants and form carcinogenic nitrosamines, increasing cancer risks.[2] Its high solubility also leads to persistent groundwater contamination, making it a pervasive and challenging environmental issue. Therefore, it is very necessary to efficiently treatment nitrate-containing wastewater before it is discharged.

Biological denitrification technology is widely used to remove nitrate from sewage due to its high efficiency, low operating cost, and no secondary pollution.[3,4] Therefore, many biological water purification devices and processes have been designed and applied to remove nitrogenous compounds, such as sequencing batch biofilm reactor (SBBR),[5] moving bed biofilm reactor (MBBR),[6–8] sequencing batch biofilter granular reactor (SBBGR)[9] and upflow anaerobic sludge blanket (UASB) reactor.[10] The UASB reactor utilizes an upward flow regime through a suspended sludge bed, where anaerobic microorganisms form granular aggregates that efficiently convert organic nitrogen and other pollutants into biogas under oxygen-free conditions. The SBBR operates by filling a sequential batch reactor with fixed media, creating alternating anoxic-aerobic environments through intermittent aeration in a time sequence to achieve nitrification and denitrification for nitrogen removal.[5] The SBBGR cultivates aerobic granular sludge within an SBR, utilizing the dissolved oxygen gradient inside the granules to achieve simultaneous nitrification and denitrification. It features high biomass concentration and strong resistance to shock loads, but requires long start-up periods and complex operational control.[11] The MBBR treats wastewater by continuously passing it through carriers in the reactor where biofilm forms, enabling microorganisms to

[a]*Department of Resources and Environmental Engineering, Shanxi Institute of Energy, Taiyuan 030000, Shanxi, China. E-mail: yangjingrui0809@126.com*
[b]*College of Safety and Emergency Management, Shanxi Vocational University of Engineering Science and Technology, Taiyuan 030619, Shanxi, China*

proliferate extensively on the carriers while degrading nitrogen-containing pollutants, thereby purifying the wastewater.[12] Comprehensive comparison demonstrates that MBBR exhibits superior performance in nitrogen removal efficiency, operational stability, resistance to shock loads, and management simplicity, making it particularly suitable for wastewater treatment scenarios with limited space and significant water quality fluctuations.[13] Therefore, MBBR was selected as the research object in this study.

However, due to the presence of an oxygen gradient inside the biofilm, dissolved oxygen (DO) is one of the key factors affecting microbial denitrification performance. Moreover, most denitrifying bacteria are heterotrophic, so they need organic carbon to provide energy, commonly expressed as the carbon-to-nitrogen (C/N) ratio, which plays a crucial role in promoting cell growth and nitrate degradation.[14,15] Therefore, the influent C/N ratio is another key parameter that directly affects microorganism's growth and denitrification efficiency.[16,17] But the C/N ratio may vary for different actual wastewater or different treatment stages. It has been reported that different C/N ratios or DO influences the denitrification performance and microbial community structure in wastewater treatment.[18,19] Previous researches have mainly attention on one of the C/N ratios or DO, but less on the effect of the interaction between C/N ratio and DO on bioreactor denitrification performance and microbial consortium structure. Because of this, we plan to designed orthogonal experiments of different C/N and DO to explore the optimal C/N and corresponding DO for MBBR, to achieve the purpose of simultaneously removing nitrate and organic pollutants efficiently.

This study aims to systematically investigate the nitrogen removal mechanisms and optimal control strategies of the highly efficient denitrifying microbial consortium HN-04, isolated from activated sludge, in a MBBR. The research first identified the optimal aerobic denitrification conditions (carbon source, C/N ratio, pH, temperature) through shake-flask experiments. Subsequently, a biofilm system was established and stabilized in the MBBR to specifically analyze the effects of different C/N ratios and DO concentrations on nitrate and organic matter degradation. Furthermore, enzyme activity assays and nitrogen balance analysis were combined to elucidate nitrate transformation pathways. Finally, high-throughput sequencing was employed to clarify the structural dynamics and functional responses of the biofilm microbial community under different operational conditions, thereby providing a theoretical foundation for the precise regulation and engineering application of MBBR processes.

2 Materials and methods

2.1 Medium

The consortium enrichment denitrifying media (EDM) contains (g L^{-1}): NaCl, 10; yeast extract, 5; peptone, 10; pH = 7.

The components of denitrification media (DM) used to nitrate treatment were as follows (g L^{-1}): $NaNO_3$, 0.607; sodium citrate, 4.20; $K_2HPO_4 \cdot 3H_2O$, 0.750; $NaH_2PO_4 \cdot 2H_2O$, 0.250; NaCl, 0.120; $MnSO_4 \cdot H_2O$, 0.010; $MgSO_4 \cdot 7H_2O$, 0.050; $FeSO_4 \cdot 7H_2O$, 0.050; pH = 7.

The solid media consists of a DM medium supplemented with 1.5% agar. Each of the chemicals used in the experiments was an analytically pure reagent, and all the medium was autoclaved at 121 °C for 20 min before use.

2.2 Enrichment and isolation of the microbial consortium

The raw water was obtained from the sewage treatment plant situated in Fengyang city (Shanxi, China), 10 mL original samples were added into a 250 mL Erlenmeyer flask containing 100 mL autoclaved sterile EDM media and then cultured in a shaker with a constant temperature of 30 °C and 120 rpm. 1 mL of suspended liquid was transferred to the fresh and same EDM media every 2 days for another two-day enrichment cycle. After three consecutive cultures, the suspended liquid was spread on a solid media by the gradient concentration dilution method, and placed in a biochemical incubator at 30 °C, picked out, and purified after visible colonies formed. The selected colonies were incubated in DM medium for 48 h and individually tested their denitrification performance. Finally, a consortium with the best denitrification performance was chosen and named HN-04, which was stored in 25% glycerol solution at −80 °C.

2.3 Assessment of nitrate removal performance of microbial consortium HN-04

Consortium HN-04 was inoculated in triplicate to 100 mL denitrification media at a proportion of 1% and cultured in a shaker at 30 °C and 120 rpm. And the uninoculated experiment was used as the control group. Sodium citrate was the carbon source, nitrate with an initial concentration of 100 mg L^{-1} was the single nitrogen source, and the C/N ratio was adjusted to 12. During cultivation, samples were periodically to measure the values of OD_{600} and pH, then the supernatant was taken by centrifuged (10 000 rpm, 10 min) to determine changes in total nitrogen (TN), nitrite nitrogen (NO_2^-–N), nitrate nitrogen (NO_3^-–N), ammonium nitrogen (NH_4^+–N) and chemical oxygen demand (COD).

2.4 Single-factor experimental study on affecting denitrification performance of microbial consortium HN-04

According to the conditions generally affecting enzyme activity, the effects of distinct carbon source, C/N ratio, initial pH, and temperature on aerobic denitrification ability of the consortium HN-04 were investigated. In different carbon source experiments, the C/N ratio of DM media was adjusted to 10, and then sodium citrate, sodium pyruvate, sodium succinate, sodium acetate, fumaric acid, and glucose were separately used as a single carbon source. The effects of various C/N ratios on denitrification ability of consortium were studied by adjusting the amount of carbon source (sodium citrate) to make the ratio of C/N of nitrate as nitrogen source reached 4, 8, 12, 16, and 20. To further investigate nitrate removal efficiency with different initial pH, the initial pH was set to 4, 5, 6, 7, 8, 9, 10, and 11 using 4 mol per L HCl or 4 mol per L NaOH. The incubation

temperature was controlled in the range of 10–45 °C. All the above experiments were performed in triplicate with 1% (v/v) inoculum amount, and the non-inoculum samples experiment were taken as controls. Unless otherwise specified, all single-factor experiments were conducted under the following standard conditions: incubation for 48 h on a shaker at 120 rpm and 30 °C; an initial nitrate concentration of 100 mg L^{-1}; a C/N ratio of 12; and an initial pH of 7.0. All shake-flask experiments were conducted using a constant temperature oscillator shaker (DHZ-CA, Taicang, China). The operational parameters of 30 °C and 120 rpm were selected based on preliminary experiments which demonstrated that this combination optimally balanced microbial growth and oxygen transfer efficiency. Specifically, 30 °C falls within the mesophilic range ideal for most wastewater-derived microorganisms, while 120 rpm on a constant temperature oscillator shaker provided sufficient mixing to maintain homogeneous conditions and adequate gas–liquid transfer without causing excessive shear stress or foam formation, thereby ensuring reproducible denitrification performance. Regularly measure the various indicators of the above experiments, including OD_{600}, pH, TN, NO_2^-–N, NO_3^-–N, NH_4^+–N and COD concentration.

2.5 Bioreactor set-up and operation strategy

In the study of the bioreactor, the effects of different C/N ratios and DO on the denitrification performance of MBBR were evaluated. The MBBR reactor was made of plexiglass with a total effective volume of 5 L (height = 100 cm, inner diameter = 8 cm). 50% of the reactor volume was filled with polyurethane foam as biofilm carriers, and the carrier was a cube with a side length of 2 cm. Air was introduced into the bottom of the bioreactor by an aeration pump. The bioreactor contained 5 L of synthetic wastewater and keeps the reactor running at 30 °C by circulating water bath. The constitution of the synthetic wastewater in the bioreactor is the same as that of DM medium except for the content of sodium citrate is different. The pH of synthetic wastewater is also 7.0. Table S1 details the operation conditions and denitrification performance of the bioreactor in different stages.

The bioreactor was run in five stages, adopting a single-reactor sequencing batch operation with no parallel blank controls; however, three samplings were performed for each condition/time point as technical replicates. The first stage (days 1–8) being the start-up and microbial membrane formation stage, as shown in Table S1. At this period, the bioreactor was started up under the best conditions determined by the single-factor experiment described above (carbon source of sodium citrate, C/N = 12, t = 30 °C, pH = 7). The inoculation dose of microbial consortium HN-04 was 2% (v/v) and DO was 0.6 mg L^{-1}. After the biofilm was successfully formed, the inoculum was no longer added to the bioreactor in Stage 2–5, only the C/N ratio and DO in the bioreactor were varied. In Stage 2–5, the effects of different C/N ratios and DO on the performance of the bioreactor were evaluated by measuring the concentration of TN, NO_2^-–N, NO_3^-–N, NH_4^+–N and COD in the effluent.

2.6 Enzyme assay at different stages

Take the microbial consortium solution at the end of each stage for centrifugation (10 000 rpm, 20 min, 4 °C), then discard the supernatant and washed three times with 0.01 mol per L phosphate buffer (pH = 7.4) to resuspend the consortium. The consortium suspensions were lysed by ultrasonic treatment for 20 min, then centrifuged (14 000 rpm, 20 min, 4 °C) to obtain the cell-free extract. Periplasmic nitrate reductase (NapA) and cytochrome cd_1-type nitrite reductase (NirS) are two key enzymes in the process of denitrification, and their activities can be detected according to the method of Wang *et al.*[20] The protein concentration of enzyme extract was measured using the Bradford Protein Assay Kit (Sangon, Shanghai, China). One unit of enzyme activity (U) was defined as the amount of enzyme which catalyzed the conversion of 1 μmol of substrate per minute. The specific activity (U per mg) was defined as the concentration of enzyme units divided by the amount of protein in a milligram. These experiments were carried out in triplicate.

2.7 Nitrogen balance analysis at different stages

On the last day of each stage, only oxygen was injected into the reactor, and the oxygen flow was controlled by a mass flow meter to reach the corresponding DO concentration. After 24 h of culture, 400 μL of gas samples were drawn from the reactor outlet and the N_2 content was detected by gas chromatography. Meanwhile, samples were collected from the reactor at 0 h and 24 h respectively, and the contents of NO_3^-–N, NO_2^-–N, NH_4^+–N and TN in the supernatant were measured after centrifugation at 1000 rpm for 10 minutes. The intracellular nitrogen content was calculated by subtracting the TN after centrifugation from the TN uncentrifuged.

2.8 DNA extraction, PCR amplification, and sequencing

Three identical biofilms (three packings) carriers were taken from the bioreactor at the end of each stage of operation. Total community genomic DNA was extracted with EZNA® Soil DNA Kit (OMEGA, USA), according to the manufacturer's instructions. We used Qubit 2.0 (life, USA) to measure DNA concentration to ensure that we extracted a sufficient amount of high-quality genomic DNA. The 16S rRNA V3–V4 hypervariable regions were amplified through PCR using forward primer 341F (CCTACGGGNGGCWGCAG) and reverse primer 805R (GACTACHVGGGTATCTAATCC). The total amplification reaction mixture was 30 μL contained 15 μL of 2×Taq master Mix, 20 ng of genomic DNA, 10 μM forward and reverse primers each 1 μL and ddH_2O. The detailed thermocycling procedures were: 1 cycle of denaturation for 3 min at 95 °C, first 5 cycles of denaturation for 30 s at 95 °C, annealing for 30 s at 45 °C, an extension for 30 s at 72 °C, followed by 20 cycles of denaturation for 30 s at 95 °C, annealing for 30 s at 55 °C, extension for 30 s at 72 °C and a final 5 min extension at 72 °C. The amplicons of each reaction mixture were combined with the same molar ratio according to its concentration. The sequencing was then carried out by the Illumina MiSeq platform (USA, Illumina MiSeq) following the manufacturer's instructions.

2.9 Analytical methods and calculations

Bacterial growth was monitored by measuring the optical density at 600 nm (OD_{600}) using a spectrophotometer (SP-752, Spectrum, Shanghai, China). The concentrations of NH_4^+–N, NO_3^-–N, NO_2^-–N, and TN were determined following standard methods (APHA, 1998).[21] Specifically, NO_2^-–N was analyzed using the *N*-(1-naphthalene)-diaminoethane method at 540 nm, and NO_3^-–N was measured by the phenol disulfonic acid method at 410 nm. The concentration of NH_4^+–N was measured by employing Nessler's reagent colorimetric method at 420 nm. TN and intracellular nitrogen were determined by alkaline persulfate oxidation followed by UV spectrophotometric detection. DO and pH were measured with a DO meter (HI98193, HANNA, Italy) and a pH meter (PB-10, Sartorius, Germany), respectively. COD was analyzed by the potassium dichromate method using a COD analyzer (DR 1010, HACH, USA).

Formulae $(C_0 - C_t)/C_0 \times 100\%$ and $(C_0 - C_t)/t$ represent the degradation efficiency and removal rate of nitrogen (NO_3^-–N and TN) and COD respectively. C_0 represents the initial nitrogen or COD concentration, C_t were concentration at time t and t was the incubation time of microbial community HN-04. All tests were performed in triplicate.

3 Results and discussion

3.1 Denitrification performance of the community HN-04

Fig. 1 depicted the microbial growth and nitrate removal characteristics of HN-04 in DM medium under the aerobic condition of oscillating culture. The HN-04 reduced the nitrate concentration from 100.1 mg L^{-1} to 2.70 mg L^{-1} within 12 h, and the degradation efficiency and maximum removal rate of nitrate reached 97.3% and 14.5 mg L^{-1} h^{-1}, respectively. Then, the nitrate concentration continued to decrease and was completely degraded within 18 h, while the OD_{600} also reached the peak value of 0.91. Notably, no ammonium accumulation was observed throughout the entire process, with the maximum ammonium concentration being only 1.25 mg L^{-1}, indicating the absence of dissimilatory nitrate reduction to ammonium (DNRA). In contrast, when consortium FG-06 used sodium succinate as carbon source and C/N was 16, only about 50% of nitrate was removed in 12 h, and the maximum removal rate of nitrate in the whole degradation process was only 4.53 mg L^{-1} h^{-1},[22] which was far lower than the nitrogen reduction capacity of HN-04. In the process of HN-04 degradation of nitrate, a significant accumulation of nitrite appeared and reaching a maximum value of 42.3 mg L^{-1} at 12 h, the accumulation of nitrite resulted in the TN removal efficiency of only 54.1%. However, when the culture time reached 18 h, the concentration of nitrite in the solution decreased to 0.024 mg L^{-1}, and the TN removal efficiency was as high as 98%, which was much higher than the 75% TN degradation efficiency of *Pseudomonas stutzeri* ZF31 in 24 h.[23] The aerobic denitrification process of *Pseudomonas stutzeri* strain XL-2 (ref. 24) and *Enterobacter cloacae* CF-S27 (ref. 25) also showed the phenomenon of nitrite accumulated first and then degraded. The order of nitrate reduction by biological denitrification is generally as follows: nitrate → nitrite → nitric oxide → nitrogen-containing gas,[1] indicating that when nitrate is the only nitrogen source, the accumulation of nitrite as an intermediate is a normal phenomenon. However, there was no nitrite accumulation during the process of nitrate degradation in some strains,[26–28] such as *Arthrobacter arilaitensis* Y-10, *Pseudomonas stutzeri* YZB-001, and *Acinetobacter* sp. Y16, which may be related to the rapid conversion of intermediate nitrite into the gas by nitrite reductase.

Moreover, the removal efficiency of COD reached 93.3% with the complete removal of nitrate in 18 h, which fully proved that the consortium HN-04 can simultaneously degrade nitrogen and organic matter. It also can be seen from the figure that denitrification mainly occurs in the logarithmic growth period of 6–18 h, and the maximum specific growth rate of the HN-04 was 0.1 h^{-1} between 6–12 h. And the pH value increased from the initial 7.0 to 9.1 with the bacterial growth, which was due to the generation of alkali during the denitrification process.[29]

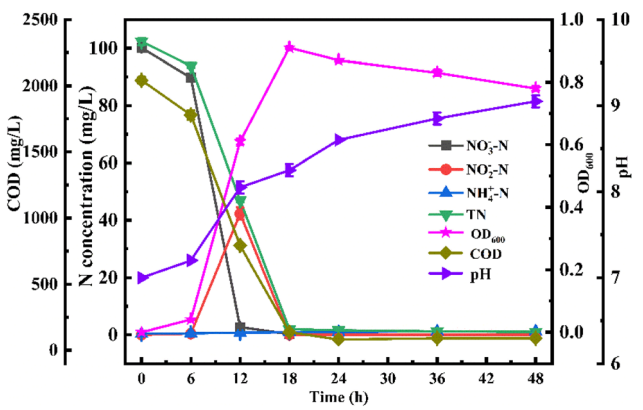

Fig. 1 Growth and denitrification performance of microbial consortium HN-04 under standard conditions (C/N ratio = 12; 30 °C; 120 rpm). Values are means ± SD (error bars) for three replicates. Lines serve as visual guides.

3.2 Effects of different influencing factors on the denitrification process of the consortium HN-04

3.2.1 Carbon source. As shown in Fig. 2a, HN-04 utilized all six tested carbon sources for growth and nitrogen removal, though with distinct nitrate degradation patterns depending on the carbon source. This variation may be attributed to differences in the oxidation/reduction potentials of different carbon sources, which ultimately influence denitrification efficiency.[30] When sodium citrate, sodium succinate, or sodium acetate served as the sole carbon source, nitrate removal efficiency exceeded 50%. Among these, sodium citrate supported the highest removal efficiencies for nitrate ($p < 0.05$), TN, and COD—reaching 94.9%, 63.6%, and 99.2%, respectively—along with the highest maximum cell density. The superior performance observed with sodium citrate may be explained by its role as an intermediate metabolite in the tricarboxylic acid (TCA) cycle, enabling direct bacterial utilization and thereby enhancing metabolic activity and shortening denitrification time. In contrast, HN-04 showed limited growth and

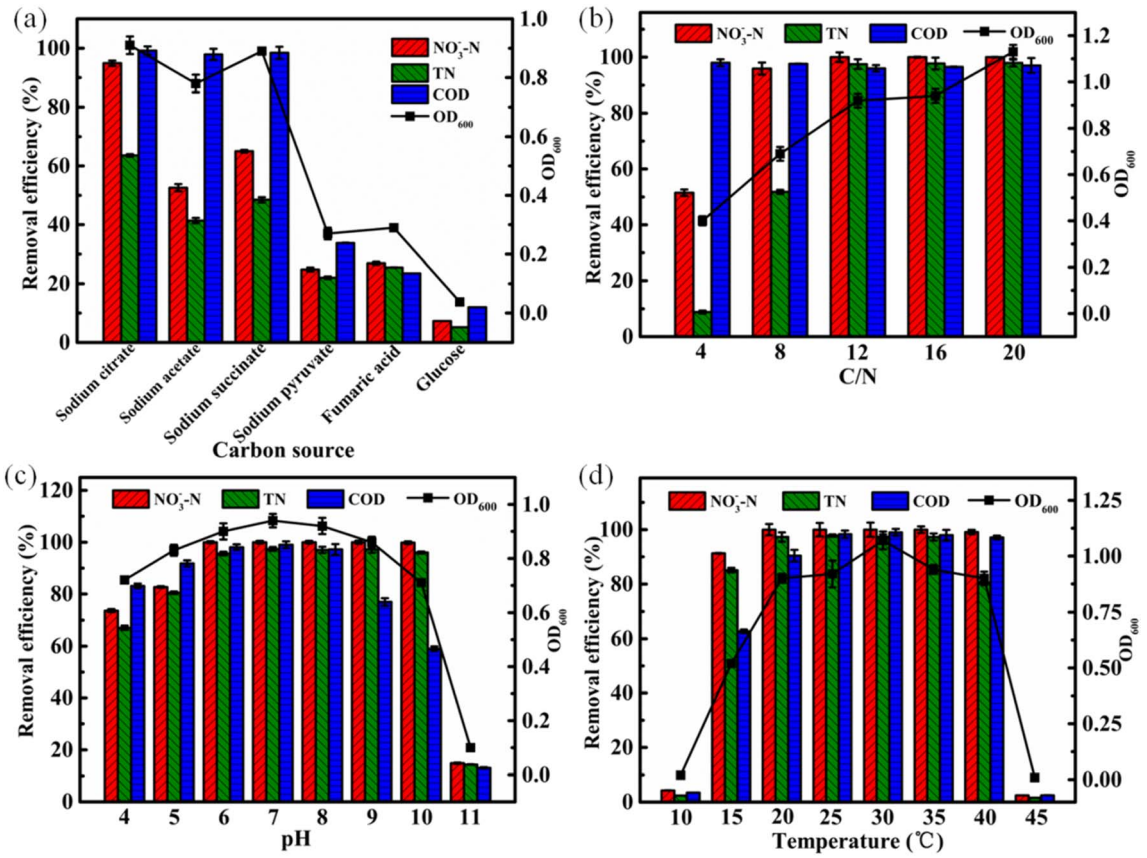

Fig. 2 Effects of carbon source (a), carbon-to-nitrogen (C/N) ratio (b), pH (c), and temperature (d) on denitrification ability of microbial consortium HN-04 in 48 h. Values are means ± SD (error bars) for three replicates. Lines serve as visual guides.

denitrification activity when sodium pyruvate, fumaric acid, or glucose were supplied as sole carbon sources. Notably, with glucose, the maximum NO_3^-–N removal efficiency was only 7.30%, and the maximum OD_{600} reached merely 0.040. These results indicate a strong correlation between bacterial growth and denitrification performance in community HN-04. Based on the above findings, sodium citrate was identified as the most suitable carbon source for supporting HN-04 growth and nitrate degradation, and was therefore selected for use in subsequent experiments in this study.

3.2.2 C/N ratio. The C/N ratio significantly influences bacterial metabolism and energy utilization. As shown in Fig. 2b, the aerobic denitrification capacity of consortium HN-04 was markedly affected by different C/N ratios ranging from 4 to 20. When the C/N ratio exceeded 12, NO_3^-–N was completely removed, and TN removal efficiency surpassed 97%. In contrast, at a C/N ratio of 4, the removal efficiencies of NO_3^-–N and TN were only 51.5% and 8.8%, respectively, which can be attributed to insufficient carbon availability for complete denitrification.[17] As the C/N ratio increased to 12, microbial denitrification efficiency improved rapidly ($p < 0.05$), likely due to enhanced cell growth and metabolic activity under carbon-sufficient conditions. However, when the C/N ratio was further increased beyond 12, NO_3^-–N removal remained complete, while TN removal efficiency showed no significant improvement ($p > 0.05$). This suggests that once the carbon supply exceeds the metabolic demand of the cells, it ceases to be a limiting factor, and bacterial growth and denitrification activity stabilize. These results demonstrate that efficient heterotrophic denitrification by HN-04 requires a C/N ratio of at least 12. Therefore, a C/N ratio of 12 was selected for subsequent experiments in this study.

3.2.3 pH. The growth and nitrate removal performance of consortium HN-04 were evaluated across a broad pH range (4–11) after incubation at 30 °C for 48 h under adjusted initial pH conditions. As shown in Fig. 2c, both microbial biomass and nitrate removal were influenced by pH variation ($p < 0.05$). Microbial growth first increased and then decreased over the pH range, with the highest OD_{600} value (0.940) observed at pH 7. Complete NO_3^-–N removal occurred between pH 6 and 10, accompanied by TN removal exceeding 95.0%. The maximum nitrate removal rate reached 10.8 mg L^{-1} h^{-1} at pH 7, while rates at other pH values (4–11) were 3.23, 4.33, 8.21, 7.67, 7.40, 5.55, and 0.760 mg L^{-1} h^{-1}, respectively. TN and COD removal trends were similar to that of nitrate, with the highest and fastest removal also occurring at pH 7. Notably, HN-04 maintained high growth activity from pH 4 to 10, demonstrating its adaptability to a wide pH range. This contrasts with *Bacillus methylotrophicus* strain L7, which shows limited growth under acidic (pH 5–6) or alkaline (pH 9–10) conditions.[31] These results confirm that the

optimal pH for HN-04 denitrification is 7, consistent with previous studies indicating that neutral to slightly alkaline conditions favor denitrifying bacterial activity.[31,32]

3.2.4 Temperature. As shown in Fig. 2d, microbial consortium HN-04 demonstrated growth and NO_3^-–N removal across a temperature range of 15–40 °C. In contrast, both OD_{600} values and NO_3^-–N concentrations showed negligible change at 10 °C or 45 °C, likely due to suppressed denitrifying enzyme activity under these temperature extremes. TN removal efficiency exceeded 85% at 15 °C and reached over 97% between 20–35 °C, but decreased to 80.5% at 40 °C, indicating high denitrification efficiency within the 20–35 °C range. Such a broad temperature adaptability enhances the ecological competitiveness and survival potential of the consortium in natural environments, supporting its effective aerobic denitrification capacity. The maximum OD_{600} value (1.07) was observed at 30 °C, accompanied by optimal growth and the strongest nitrogen removal performance, with removal efficiencies of NO_3^-–N, TN, and COD reaching 100%, 97.4%, and 99%, respectively. Therefore, 30 °C was identified as the optimal temperature for NO_3^-–N removal by consortium HN-04, consistent with previous studies reporting that most aerobic denitrification processes occur optimally between 30–37 °C.[27,33,34]

3.3 Effects of different C/N ratios and DO on denitrification performance of the bioreactor

3.3.1 Startup of the MBBR and biofilm formation. The bioreactor was started under the optimum conditions determined by single-factor experiments. In the initial stage of bioreactor start-up, 100 mL fresh HN-04 consortium solution was added to the bioreactor every day until a large amount of light yellow biomass could be macroscopic observed on the surface of the polyurethane foam carriers. SEM images were used to observe the morphology of consortium grown on moving bed biofilm carriers after 8 days of initiation. Fig. S1 showed the contrast images of the biofilm carrier before and after biofilm formation. As depicted in the images, the surface of the biofilm in the experimental group was covered with a large number of microorganisms (Fig. S1b) compared with the original biofilm sample (Fig. S1a). These results indicated that the MBBR can be started quickly by inoculating microbial consortium HN-04. However, many MBBRs used for wastewater denitrification have the problem of long start-up time,[35,36] which may be related to the types of fillers and microorganisms.

3.3.2 Denitrification performance of the MBBR in different stages. Throughout the 40-day experimental run, the operational conditions of the MBBR system were regulated across five stages (Stage 1–5) to investigate the combined effects of C/N ratio and DO on the nitrogen removal performance of the system. It is noteworthy that no ammonium accumulation was observed throughout the entire operation, with ammonium concentration consistently maintained below 1.0 mg L^{-1} in the effluent, confirming complete denitrification without diversion to DNRA. The specific operational parameters and treatment efficiencies are shown in Fig. 3 (see also Table S1). During the inoculation stage (Stage 1), the concentration of nitrate in the effluent of the bioreactor was almost zero for days 2 to 8, and the removal efficiency of COD was all above 96% except the first day. In Stage 2, the nitrate removal had remained stable, but the average COD removal efficiency had dropped to 73.2% compared to 96.7% of Stage 1. The reason may be that the DO content in the bioreactor is 0.6 mg L^{-1} both in Stage 2 and Stage 1, which belongs to an anoxic environment. However, no additional bacterial solution was added in Stage 2, resulting in less organic matter needed by microorganisms than in Stage 1, and ultimately reducing the removal efficiency of organic matter. Therefore, in Stage 3, the C/N ratio was switched from 12 to 5 with DO unchanged in the bioreactor. The applied low C/N ratio conditions not only showed no adverse effect on the removal efficiency of nitrate but also improved the COD average removal efficiency from 73.2% to 97.1%. The simultaneous high-efficiency degradation of nitrogen and organic matter was realized. These results indicated that under anoxic conditions, microorganisms need fewer organic substances for self-propagation and removal of pollutants. The denitrification performance of the MBBR process at high C/N and low C/N ratios under anoxic conditions was evaluated in Stage 2 and Stage 3 respectively. Starting from Stage 4, the oxygen supply was increased to convert the bioreactor from an anoxic condition to an aerobic state, that is, the DO was increased from the original 0.6 mg L^{-1} to 3.0 mg L^{-1}. In this stage, the COD was nearly completely removed, while only about 68.6% of nitrate was reduced. It is noteworthy that the improvement of DO not only resulted in the increased the concentration of NO_3^-–N in the effluent, but also an increase of NO_2^-–N average concentration in the effluent to 32.3 mg L^{-1}. Whereas the NO_2^-–N concentration in the effluent of the first three stages of the operation period was <0.05 mg L^{-1}. Indicating that the combined effect of high DO and low C/N ratio severely inhibited the denitrification process, particularly the activity of nitrite reductase. Partial removal of nitrate and accumulation of nitrite maybe since under conditions of insufficient electron donor (COD), oxygen inhibits denitrification by providing a better electron acceptor, allowing the denitrification population to produce energy, leading to a decrease in denitrification activity and accumulation of nitrogenous intermediates under conditions of high DO.[37,38] To prove the point, the C/N ratio in the bioreactor was switched back to 12 under aerobic conditions (Stage 5), and the COD removal efficiency was steady at 96.3% at this stage. However, the removal efficiency of NO_3^-–N and TN increased significantly with the increase of the C/N ratio from 5 to 12 ($p < 0.05$). It not only caused the degradation efficiency of NO_3^-–N reach 100%, but also made the NO_2^-–N concentration in the effluent was almost zero. A NO_3^-–N removal rate of 4.22 mg L^{-1} h^{-1} was maintained in the reactor during this operational phase. These results were similar to those reported by Nguyen *et al.*[39] and Mousavi *et al.*[40] for an increase in the C/N ratio. This could be explained by the that heterotrophic bacteria work well under aerobic conditions when sufficient carbon sources were available. This further verifies that an appropriate C/N ratio can effectively alleviate the inhibitory effect of high DO on denitrification, thereby achieving complete denitrification. In summary, the synergistic interaction between C/N ratio and DO is a critical factor determining the denitrification performance and intermediate accumulation in the MBBR system. The combination of low C/N ratio and high DO readily

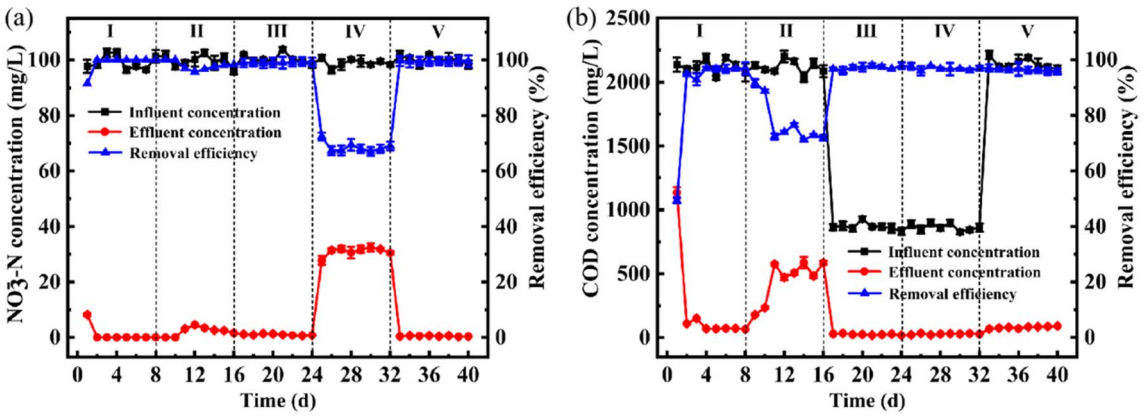

Fig. 3 Performance in MBBR at five different stages: (a) nitrate removal, (b) chemical oxygen demand (COD) removal. Values are means ± SD (error bars) for three replicates. Lines serve as visual guides.

leads to incomplete denitrification and nitrite accumulation, while increasing the C/N ratio can effectively restore the system's nitrogen removal efficiency. The organic carbon demand of heterotrophic denitrifying microorganisms demonstrates a positive correlation with the ambient dissolved oxygen concentration.

3.4 Removal pathway of nitrate by the microbial consortium in MBBR

To investigate the removal pathway of nitrate by microbial community in MBBR, the activities of two key enzymes in the denitrification process, NapA and NirS in five different stages were evaluated. As shown in Fig. 4, the activities of the two enzymes varied across different operational phases, with both NapA and NirS reaching their peak activities in Stage 3 at 0.170 U mg^{-1} and 0.285 U per mg protein, respectively. These enzymatic activity patterns align with the expression levels of nitrate reductase genes and nitrite reductase genes reported in multiple studies. For instance, Liu *et al.* observed significantly higher narG gene abundance in the biofilm carriers of a magnetic carrier-enhanced MBBR system during high-efficiency denitrification phases compared to the initial sludge.[41] The synchronized enhancement of NapA and NirS activities observed in our study during the equally efficient denitrification phase indicates that consortium HN-04 similarly enriched bacterial strains possessing complete denitrification capabilities, demonstrating functional potential comparable to high-efficiency communities identified through genetic sequencing. Furthermore, the activities of the two enzymes were significantly higher at a low C/N ratio than at a high C/N ratio ($p < 0.05$), so we speculated that the high organic load might have a certain inhibitory effect on the activity of the two enzymes. The responsive pattern of these enzymatic activities to identical environmental stressors functionally reinforces the conclusion that carbon source availability serves as a core factor regulating the denitrification potential in MBBR systems. Besides, N_2 was detected in gaseous denitrification products at each stage. This indicates that consortium HN-04 possesses the capability to completely reduce nitrate to nitrogen gas, minimizing the intermediate accumulation risk of greenhouse gas N_2O, which is of great significance for environmental safety in engineering practice. Table 1 presents the nitrogen balance analysis results in MBBR at different stages. The results showed that 78.1% of nitrogen was discharged as gaseous product N_2 in Stage 3, and 15.9% of nitrogen was used for cell synthesis and converted to biomass. Compared with other studies, N_2 produced by microorganisms in MBBR during Stage 3 operation was significantly higher than that of several aerobic denitrifiers, such as 71.88% for *Paracoccus denitrificans* Z195,[42] 55.47% for *Pseudomonas* sp. JQ-H3.[43] However, strain Z195 and JQ-H3 transformed 20.53% and 38.22% of nitrogen into biomass respectively, which was much higher than that of microorganisms in Stage 3. The results showed that the microorganisms in MBBR operation Stage 3 have the characteristics of high nitrogen loss rate and low biomass production, which is beneficial to wastewater treatment and sludge reduction in a low C/N ratio and anoxic environment.

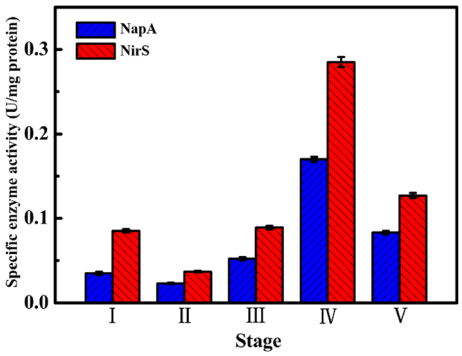

Fig. 4 Activities of periplasmic nitrate reductase (NapA) and cytochrome cd_1-type nitrite reductase (NirS) in five different operating stages. Values are means ± SD (error bars) for three replicates.

In summary, it is speculated that there are two nitrate removal pathways for microorganisms in MBBR, one of which is as follows: NO_3^-–N → NO_2^-–N → NO → N_2O → N_2. This nitrate removal pathway was consistent with the denitrification path reported by Huang *et al.*[23] The other is the conversion to biomass nitrogen through microbial assimilation.

Table 1 Nitrogen balance in different operational stages of MBBR

Stages	Initial NO_3^-–N (mg L^{-1})	Final nitrogen concentrations (mg L^{-1})					
		NO_3^-–N	NO_2^-–N	NH_4^+–N	Intracellular-N	N_2	Lost N (%)
1	101.3	0	0.050	1.29	52.4	39.0	8.5
2	97.5	1.61	0.030	1.57	34.3	54.2	5.94
3	98.3	0.756	0.020	0.93	15.6	76.8	4.27
4	98.8	30.5	31.8	1.21	13.2	18.5	3.63
5	99.6	0.390	0.043	1.11	30.8	63.4	3.87

3.5 Microbial community analyses of MBBR in different operation stages

3.5.1 Diversity and richness of microbial community. Combined with the denitrification performance of the MBBR under different C/N ratios and DO conditions mentioned above, the representative biofilm samples (T0–T4) in Stage 1–5 were analyzed by high-throughput sequencing, to further understand the changes of microbial community structure in the MBBR. Table 2 exhibited the Alpha indices of five samples, and the species richness and diversity of the sample microbial consortium were estimated by a series of statistical analysis indices. The coverage indices reflected that almost all of the OTU sequences in the five samples were measured. The Chao1 and ACE indices indicating the richness estimator of communities, Shannon and Simpson index implying the diversity of bacterial communities. The number of high-quality reads in five samples ranged from 67 296 to 164 990. The larger OTUs number in bacterial sequences along with the ACE and Chao1 indices indicating that community richness in T0 was highest, whereas Shannon and Simpson's index jointly implied the T0 lower diversity of bacterial communities than other samples.[44] The Shannon and Simpson indices revealed that during the stable operational phases (T1–T4) of the MBBR, microbial diversity was higher under conditions with elevated C/N ratios. This observation aligns with the general trend reported by Chen *et al.*,[45] which reported that as the C/N ratio increased from 3 to 9, microbial community diversity and richness reached their highest levels, as demonstrated by the Shannon, Simpson, ACE, and Chao1 indices. However, our findings extend beyond this range, demonstrating that high diversity can be maintained at even higher C/N levels. Gu *et al.*[46] have pointed out that the number of OTUs with abundant differences in the high C/N ratio was higher than that with a low C/N ratio. In our research, the number of differentially abundant OTU of the T2 sample was relatively high, probably because the abundance of community was not only related to C/N but also the corresponding DO content. Furthermore, we also found that during the MBBR stabilization phase (T1–T4), the richness of the community was higher when the bioreactor performance was better (T2 and T4). This fully shows that the microbial community structure in MBBR is closely related to the denitrification process.

3.5.2 Composition and change of microbial community. The microbial community composition and dynamics in biofilm samples (T0–T4) from the MBBR under varying C/N ratios and DO conditions were analyzed using high-throughput sequencing. As shown in Fig. 5a, 26 phyla were identified across all samples, with four phyla common to all five sampling points. *Proteobacteria*, *Bacteroidetes*, and *Firmicutes* dominated throughout the operational period, the sum of three phyla accounted for 99.98% (T0), 98.72% (T1), 98.5% (T2), 98.59% (T3), and 99.85% (T4) of the total reads. *Proteobacteria* and *Bacteroidetes* exhibited the highest relative abundance, consistent with findings reported by Gu *et al.*[46] The relative abundance of *Proteobacteria* reached 98.98% at the start-up stage (T0), then decreased throughout the stabilization period (T1–T4), though it remained above 47%. This aligns with numerous studies identifying *Proteobacteria* as a dominant denitrifying phylum in wastewater treatment systems.[47–49] Notably, the relative abundance of Bacteroidetes peaked at 50.95% in Stage 4 (T3, C/N = 5, DO = 0.6 mg L^{-1}) and was lowest at 0.99% in Stage 1 (T0). Furthermore, *Bacteroidetes* abundance was consistently higher under C/N = 5 than under C/N = 12, suggesting that low C/N conditions favor its proliferation. In contrast, *Firmicutes* were nearly undetectable during start-up (0.01%) but increased during stable operation (0.29–11.55%). These results demonstrate that while variations in C/N ratio and DO did not alter the taxonomic diversity at the phylum level, they significantly influenced the relative abundance of dominant phyla, thereby shaping the microbial community structure in the MBBR system.

Fig. 5b showed the relative abundance distribution of microbial communities at the class level across the five samples. The dominant classes consistently observed included

Table 2 Microbial statistical analysis of five samples in different operational stages of MBBR

Sample	Reads	OTU	Shannon	ACE	Chao1	Coverage	Simpson
T0	138 245	1080	1.42	14 462.85	5707.88	0.99	0.38
T1	94 041	568	2.94	3158.48	1956.47	1.00	0.09
T2	93 546	938	1.93	4920.24	2771.15	0.99	0.35
T3	67 296	437	2.41	3813.17	1418.28	1.00	0.21
T4	164 990	854	2.78	5574.40	3074.67	1.00	0.14

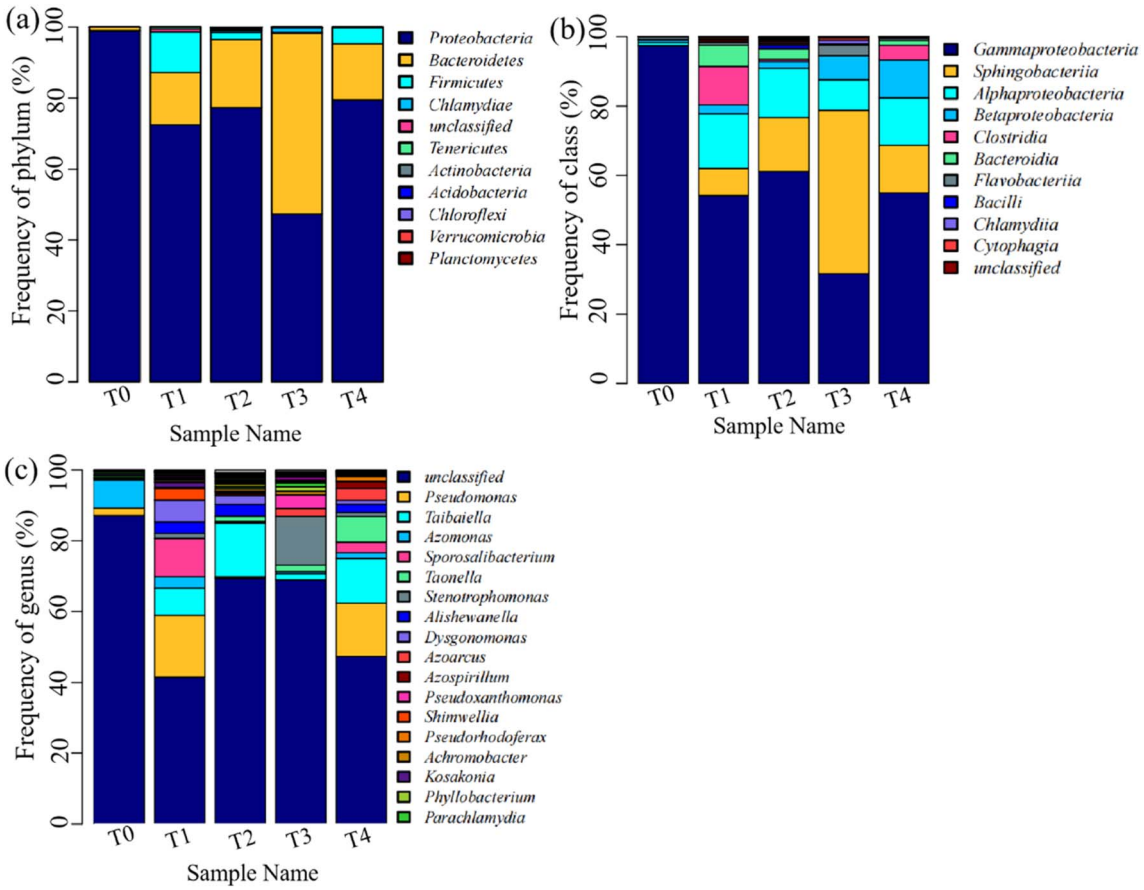

Fig. 5 Bacterial community composition and relative abundance at (a) phylum, (b) class, and (c) genus levels.

Gammaproteobacteria (31.71–97.34%), *Sphingobacteriia* (0.09–47.08%), *Alphaproteobacteria* (0.8–15.76%), and *Betaproteobacteria* (0.83–10.8%), *Gammaproteobacteria* remained the predominant class shared among all samples, while *Alphaproteobacteria* emerged as another dominant class during the stable operational phases (T1–T4). These findings align with the research of Lu *et al.*,[38] who noted that both *Gammaproteobacteria* and *Alphaproteobacteria* belonged to sub-*Proteobacteria*—exhibit remarkable aerobic denitrification capabilities. Additionally, the substantial proportion (0.09–47.08%) of *Sphingobacteriia* during stable MBBR operation corroborates earlier studies reporting the involvement of this denitrifying class in nitrogen removal processes.[50] A gradual increase in the relative abundance of *Betaproteobacteria* (0.83–10.8%) was also observed, consistent with previous reports of its prevalence in biofilm systems within MBBR-based wastewater treatment.[51,52]

As shown in Fig. 5c, significant differences were observed among samples at the genus level. A total of 48 genera were identified across all samples. During the start-up phase (T0), *Azomonas* (7.96%) and *Pseudomonas* (2.13%) were the main classified genera, alongside a substantial proportion (87.15%) of unclassified sequences. The microbial composition shifted substantially during subsequent operational phases. In sample T1, the dominant genera included *Pseudomonas* (17.43%), *Taibaiella* (7.67%), *Azomonas* (3.19%), *Sporosalibacterium* (10.78%), *Alishewanella* (3.28%), *Dysgonomonas* (6.13%), and *Shimwellia* (3.22%). Sample T2 showed a marked increase in *Taibaiella* (15.16%), establishing it as the dominant genus. A notable enrichment of the aerobic bacterium *Stenotrophomonas* (13.81%) was observed in sample T3. Under high C/N ratio and aerobic conditions (T4), *Pseudomonas* (15.09%), *Taibaiella* (12.54%), and *Taonella* (7.3%) emerged as the major genera. It is noteworthy that the relative abundance of *Pseudomonas* was significantly lower at C/N = 5 (T2 and T3). This genus has been widely reported as a key denitrifying microorganism in both activated sludge and biofilm systems under various environmental conditions.[53–55] Additionally, several less abundant genera were detected, including known denitrifiers such as *Azoarcus*, *Comamonas*, and *Aeromonas*, which have been documented in previous studies.[56–59] These results demonstrate that variations in C/N ratio and DO concentration drive structural reorganization of microbial communities in MBBR biofilms, while maintaining a functional core comprised of established denitrifying bacteria.

4 Conclusions

This study systematically elucidated the synergistic regulatory mechanism of C/N ratio and DO on the denitrification performance and microbial community structure of the MBBR. The

experimental results showed that when the C/N was 12 and the DO was maintained at 2.0 mg L^{-1}, the system achieved optimal performance, with total nitrogen and organic matter removal efficiencies exceeding 96%, along with highly efficient denitrification. These conditions not only provided sufficient carbon sources for denitrifying bacteria but also created an ideal oxygen gradient microenvironment within the biofilm, significantly enriching core denitrifying phyla including *Proteobacteria*, *Bacteroidota*, and *Firmicutes*. The research confirms that the microbial community structure is highly sensitive to changes in operational parameters, and its succession pattern shows a significant positive correlation with system denitrification performance. Furthermore, the experiment revealed two nitrate removal pathways in the MBBR: microbial assimilation and denitrification. These findings provide important theoretical foundation and practical guidance for the precise regulation of MBBR processes in treating low C/N wastewater.

Conflicts of interest

There are no conflicts to declare.

Data availability

The authors confirm that the data supporting the findings of this study are available within the article and its supplementary information (SI). Supplementary information is available. See DOI: https://doi.org/10.1039/d5ra02142a.

Acknowledgements

This study was financially supported by the Basic Research Program Project of Shanxi (Grant No. 202203021212474), and the Scientific and Technological Innovation Programs of Higher Education Institutions in Shanxi (Grant No. 2022L606).

References

1 H. Guo, J. Wu, J. Lian, B. Chen, G. Meng, Y. Wang, M. Shen, Q. Kong and H. Wu, *J. Environ. Chem. Eng.*, 2025, **13**(3), 116668.
2 B. Muththamizh, A. Sowmya and M. Rajesh, *Int. J. Biol. Macromol.*, 2025, **304**(P1), 140843.
3 I. Zekker, E. Rikmann, T. Tenno, A. Seiman, L. Loorits, K. Kroon, M. Tomingas, P. Vabamäe and T. Tenno, *Environ. Technol.*, 2014, **35**(9–12), 1565–1576.
4 Z. Chai, W. Yao, H. Chen, Y. He and M. Zheng, *J. Environ. Manage.*, 2025, **393**, 127024.
5 S. Liu, X. Han, M. Zhou, Y. Gao, Y. Zhang, Q. Li, N. Guo, J. Hua, J. Kang and G. Song, *Water, Air, Soil Pollut.*, 2025, **236**(11), 702.
6 X. Fan, J. Wang, X. Wang, D. Wu, H. Liu, X. Zhou, S. Huang, J. Zhou, W. Han and X. Liu, *J. Environ. Chem. Eng.*, 2025, **13**(5), 118519.
7 I. Zekker, E. Rikmann, T. Tenno, A. Saluste, M. Tomingas, A. Menert, L. Loorits, V. Lemmiksoo and T. Tenno, *Environ. Technol.*, 2012, **33**(4–6), 703–710.
8 I. Zekker, E. Rikmann, T. Tenno, P. Vabamäe, K. Kroon, L. Loorits, A. Saluste and T. Tenno, *Environ. Technol.*, 2012, **33**(20), 2263–2271.
9 E. Barca, M. De Sanctis, V. G. Altieri and C. Di Iaconi, *Energy Convers. Manage.*, 2020, **228**, 113582.
10 I. Zekker, E. Rikmann, T. Tenno, K. Kroon, A. Seiman, L. Loorits, H. Fritze, T. Tuomivirta, P. Vabamäe, M. Raudkivi, A. Mandel and T. Tenno, *Environ. Technol.*, 2015, **36**(1–4), 214–225.
11 C. Di Iaconi, M. De Sanctis, S. Rossetti and R. Ramadori, *Water Sci. Technol.*, 2008, **58**(2), 367–372.
12 Y. Quan, H. Wang, Q. Hang, Y. Deng, K. Liu, C. Li and S. Zheng, *Environ. Sci. Pollut. Res.*, 2015, **22**(18), 13970–13979.
13 J. Li, S. Tabassum, G. L. Li and H. Altundag, *J. Water Process Eng.*, 2025, **73**, 107688.
14 K. C. Lee and B. E. Rittmann, *Water Res.*, 2003, **37**(7), 1551–1556.
15 Z. Xu, X. Dai and X. Chai, *Sci. Total Environ.*, 2018, **634**, 195–204.
16 X. Chen, Q. Zhang, Y. Zhu and T. Zhao, *Bioresour. Technol.*, 2021, **336**, 125339.
17 H. Zhong, L. Dong, Y. Tang, L. Qi and M. Wang, *Water*, 2023, **15**(24), 4298.
18 Y. Gu, Y. Wei, Q. Xiang, K. Zhao, X. Yu, X. Zhang, C. Li, Q. Chen, H. Xiao and X. Zhang, *Sci. Total Environ.*, 2019, **651**(P1), 625–633.
19 T. N. P. Nguyen, S. J. Chao, P. C. Chen and C. Huang, *J. Environ. Sci.*, 2018, **69**(07), 52–60.
20 Y. Wang, H. Chen, Y. X. Liu, R. P. Ren and Y. K. Lv, *Bioresour. Technol.*, 2016, **211**, 711–719.
21 J. R. Yang, Y. Wang, H. Chen and Y. K. Lyu, *Bioresour. Technol.*, 2019, **274**, 56–64.
22 Y. Yang, Y. Liu, T. Yang and Y. Lv, *Biochem. Eng. J.*, 2017, **120**, 33–40.
23 T. Huang, L. Guo, H. Zhang, J. Su, G. Wen and K. Zhang, *Bioresour. Technol.*, 2015, **196**, 209–216.
24 B. Zhao, D. Y. Cheng, P. Tan, Q. An and J. S. Guo, *Bioresour. Technol.*, 2018, **250**, 564–573.
25 P. Soumesh Kumar, T. Swetaleena, M. Sriprakash and M. Nikhil Kumar, *Bioresour. Technol.*, 2017, **232**, 285–296.
26 X. Huang, W. Li, D. Zhang and W. Qin, *Bioresour. Technol.*, 2013, **146**, 44–50.
27 J. Zhang, P. Wu, B. Hao and Z. Yu, *Bioresour. Technol.*, 2011, **102**(21), 9866–9869.
28 T. He, D. Xie, Z. Li, J. Ni and Q. Sun, *Bioresour. Technol.*, 2017, **239**, 66–73.
29 L. Zhu, W. Ding, L. J. Feng, Y. Kong, J. Xu and X. Y. Xu, *Bioresour. Technol.*, 2012, **108**, 1–7.
30 C. Li, J. Yang, X. Wang, E. Wang, B. Li, R. He and H. Yuan, *Bioresour. Technol.*, 2015, **182**, 18–25.
31 Q. L. Zhang, Y. Liu, G. M. Ai, L. L. Miao, H. Y. Zheng and Z. P. Liu, *Bioresour. Technol.*, 2012, **108**, 35–44.
32 H. S. Joo, M. Hirai and M. Shoda, *J. Biosci. Bioeng.*, 2007, **103**(1), 66–73.
33 Y. Liu, G. M. Ai, L. L. Miao and Z. P. Liu, *Bioresour. Technol.*, 2016, **206**, 9–15.

34 P. R. Rout, P. Bhunia and R. R. Dash, *Bioresour. Technol.*, 2017, **244**, 484–495.
35 D. Liu, C. Li, H. Guo, X. Kong, L. Lan, H. Xu, S. Zhu and Z. Ye, *Chemosphere*, 2019, **218**, 696–704.
36 Q. Yuan, H. Wang, Q. Hang, Y. Deng, K. Liu, C. Li and S. Zheng, *Environ. Sci. Pollut. Res.*, 2015, **22**(18), 13970–13979.
37 X. J. Xu, B. Shao, C. Chen, R. C. Zhang, P. Xie, X. T. Wang, Y. Yuan, A. J. Wang, D. J. Lee and Y. X. Yuan, *Chemosphere*, 2018, **212**, 837–844.
38 H. Lu, K. Chandran and D. Stensel, *Water Res.*, 2014, **64**, 237–254.
39 T. N. P. Nguyen, S. J. Chao, P. C. Chen and C. Huang, *J. Environ. Sci.*, 2018, **69**, 52–60.
40 S. Mousavi, S. Ibrahim and M. K. Aroua, *Water Environ. J.*, 2014, **28**(4), 556–565.
41 C. Liu, Q. Li, Z. Y. Song, P. Hu, S. Y. Jing and W. P. Li, *Environ. Sci.*, 2023, **44**(02), 889–899.
42 H. Zhang, S. Li, B. Ma, T. Huang, H. Qiu, Z. Zhao, X. Huang and K. Liu, *Bioresour. Technol.*, 2020, **307**, 123230.
43 X. Wang, W. Wang, Y. Zhang, Z. Sun, J. Zhang, G. Chen and J. Li, *Bioresour. Technol.*, 2019, **288**, 121506.
44 H. Qiu, W. Zhao, Z. Zhao, M. Bai, X. Bi, X. Zhou, Y. Wang, S. Su, Y. Qin and C. Wang, *J. Water Process Eng.*, 2025, **76**, 108285.
45 M. Chen, X. Zhu, D. Yan, Y. Teng, G. Zhang, Y. Li, Q. Chen, Y. Jiao, X. Xie and S. Li, *J. Environ. Chem. Eng.*, 2025, **13**(2), 115820.
46 Y. Gu, Y. Wei, Q. Xiang, K. Zhao, X. Yu, X. Zhang, C. Li, Q. Chen, H. Xiao and X. Zhang, *Sci. Total Environ.*, 2019, **651**, 625–633.
47 J. Luo, H. Liang, L. Yan, J. Ma, Y. Yang and G. Li, *Bioresour. Technol.*, 2013, **148**, 189–195.
48 L. Ye, T. Zhang, T. Wang and Z. Fang, *Environ. Sci. Technol.*, 2012, **46**(24), 13244–13252.
49 F. Han, W. Ye, D. Wei, W. Xu, B. Du and Q. Wei, *Bioresour. Technol.*, 2018, **270**, 156–165.
50 D. Chen, H. Wang, B. Ji, K. Yang, L. Wei and Y. Jiang, *Process Biochem.*, 2015, **50**(11), 1904–1910.
51 K. Kimura, N. Yamato, H. Yamamura and Y. Watanabe, *Environ. Sci. Technol.*, 2005, **39**(16), 6293–6299.
52 R. Zhang, L. Wang, P. Chen and Y. Pu, *RSC Adv.*, 2018, **8**, 37462–37471.
53 Y. Liao, L. Yang, T. He, C. Zheng, M. Zhang and L. Lu, *Bioresour. Technol.*, 2025, 133565.
54 S. S. Balsam, A. Conaway, D. L. Mould, F. J. Pierre and D. A. Hogan, *Microbiol. Spectr.*, 2025, e0068225.
55 S. Shen, Y. Zhou, H. Cheng, H. Qian, J. Wen, C. Lin and X. Lai, *Sci. Total Environ.*, 2025, **996**, 180187.
56 Q. Liu, C. Huang, X. Chen, Y. Wu, S. Lv and A. Wang, *Environ. Res.*, 2020, **188**, 109708.
57 R. Huo, W. Li, Y. Di and S. Zhou, *J. Water Process Eng.*, 2025, **72**, 107474.
58 J. F. Su, S. Yang, T. L. Huang, M. Li, J. R. Liu and Y. X. Yao, *Environ. Pollut.*, 2020, **256**(C), 113294.
59 M. Chen, W. Wang, Y. Feng, X. Zhu, H. Zhou, Z. Tan and X. Li, *Bioresour. Technol.*, 2014, **167**, 456–461.